Bridging the gap between porphyrins and porphycenes: Substituent position-sensitive tautomerism and photophysics in *meso*-diphenyloctaethylporphyrins

Sylwester Gawinkowski,[a] Grażyna Orzanowska, [a] Katarzyna Izdebska,[a] Mathias O. Senge,*[,b] and Jacek Waluk*[a,c]

Abstract: 2,3,7,8,12,13,17,18-octaethyl-5,15-diphenylporphyrin (**1**) is characterized by an inner cavity with a rectangular shape and small NH⋯N distances. It resembles porphycene, a constitutional isomer of porphyrin known for its strong intramolecular hydrogen bonds and rapid tautomerization. Such distortion of the porphyrin cavity leads to tautomeric properties of **1** which are intermediate between those of porphyrin and porphycene. In particular, a tautomerization in the lowest excited singlet state of **1** has been discovered, occurring with a rate 3 orders of magnitude lower than in porphycene, but 3-4 orders of magnitude higher than in porphyrin. An isomer of **1**, 2,3,7,8,12,13,17,18-octaethyl-5,10-diphenylporphyrin (**2**) exhibits a different kind of geometry distortion. This molecule is nonplanar, but the inner cavity shape and dimensions are similar to those of the parent porphyrin. The same hydrogen bonding strength as in porphyrin is observed for **2**. In contrast, the nonplanarity of **2** significantly influences the photophysics, leading to a decrease in fluorescence quantum yield and lifetime. Absorption, magnetic circular dichroism, and fluorescence spectra are similar for **1** and **2** and resemble those of parent porphyrin. This is a consequence of comparable energy splittings of the frontier orbitals, ΔHOMO ≈ ΔLUMO. The results demonstrate that judicious selection of substituents and their position enables a controlled modification of geometry, hydrogen bonding strength, tautomerization rate, and photophysical and spectral parameters of porphyrinoids.

Introduction

The current interest in porphyrin research is epitomized in the subtitle of the recently published *Handbook of Porphyrin Science* multiple volume series: *with Applications to Chemistry, Physics, Materials Science, Engineering, Biology and Medicine.*[1] New synthetic strategies are being designed to target such important areas as energy and information storage, catalysis, sensor design, photodynamic therapy, or imaging. Naturally, the most general goal of fundamental research on porphyrins is to understand the structure-property-reactivity relationships. For instance, it is well known that the electronic absorption spectra of porphyrins can be strongly modified by suitable substituents. In turn, photophysical properties, in particular the relative values of radiative and nonradiative depopulation rate constants, are very different for planar and nonplanar porphyrinoids.[2-4] An area closely related to porphyrin research encompasess investigations of porphyrin isomers.[5-8] The first constitutional isomer, porphycene (Scheme 1) was synthesized in 1986.[9] Four more isomers have been obtained since that time: hemiporphycene,[10, 11] corrphycene,[12, 13] isoporphycene,[14, 15] and "inverted" ("confused") porphyrin.[16, 17] Thus far, the research has been dominated by studies on porphycenes. The spectral and photophysical properties of these compounds make them very promising candidates for use in photodynamic therapy.[18, 19] For instance, electronic absorption of porphycenes in the physiologically important red region of the visible region is much stronger than in porphyrins. Fluorescence of porphycenes is usually stronger, too, albeit it can be decreased by specific alkyl substitution. Moreover, the emission intensity of *meso*-substituted porphycenes is solvent-viscosity dependent,[20] which opens the possibility to use these compounds as sensors.

The basic structural difference between porphyrin and porphycene relates to the shape and dimensions of the inner cavity composed of four nitrogen atoms sharing two protons via intramolecular hydrogen bonds (HBs). The cavity is square-like in the parent porphyrin, but rectangular in porphycene. The distance between the H-bonded nitrogen atoms is shorter in porphycene than in porphyrin (263 vs. 291 pm, respectively), whereas the NHN angle

[a]   S. Gawinkowski, G. Orzanowska, K. Izdebska, Prof. Dr. J. Waluk
       Institute of Physical Chemistry, Polish Academy of Sciences, Kasprzaka 44, 01-224 Warsaw, Poland
       E-mail: waluk@ichf.edu.pl

[b]   Prof. Dr. M. O. Senge
       School of Chemistry, SFI Tetrapyrrole Laboratory,
       Trinity College Dublin, Dublin 2, Ireland
       E-mail: sengem@tcd.ie

[c]   Prof. Dr. J. Waluk
       Faculty of Mathematics and Natural Sciences, College of Science, Cardinal Stefan Wyszyński University, Dewajtis 5, 01-815 Warsaw, Poland

is larger (152° vs. 116°).[9, 21-23] This leads to the HBs being much stronger in porphycene. This difference has a significant effect on the mechanism and rate constant of tautomerism in the two isomers. The two internal hydrogens move back and forth between two chemically equivalent *trans* tautomeric forms with a rate which is about seven orders of magnitude larger for porphycene.[24] Moreover, the transfer of two hydrogens seems to proceed in a concerted fashion in porphycene, whereas in porphyrin the reaction involves first a single hydrogen transfer, resulting in the formation of a *cis* tautomeric form; it may then undergo the transfer of the second hydrogen or return to the initial structure.[25-27]
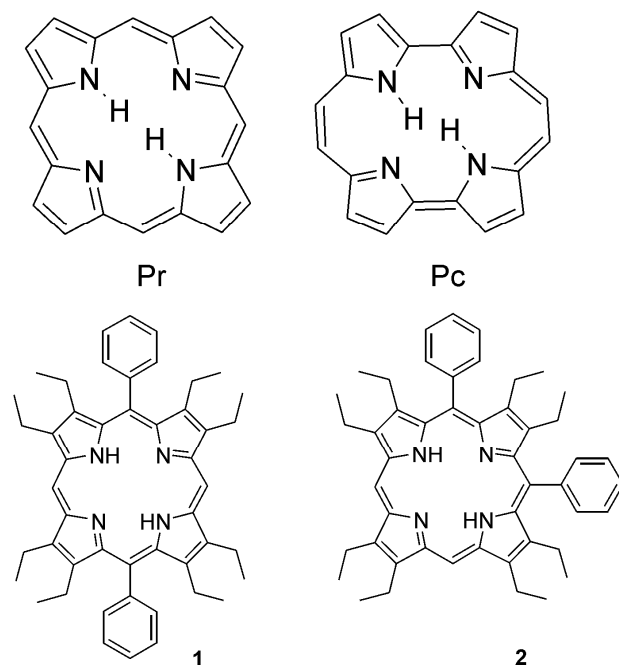
Scheme 1. Porphyrin (Pr), porphycene (Pc), 2,3,7,8,12,13,17,18-octaethyl-5,15-diphenylporphyrin (**1**) and 2,3,7,8,12,13,17,18-octaethyl-5,10-diphenylporphyrin (**2**).

In order to elucidate differences in the tautomerism one could postulate different electron density distribution in the two isomers. However, an alternative rationalization is also possible, based on geometrical factors: Even for similar electron density distributions, the hydrogen bond properties may be very different for different NH⋯N distances and/or angles. In order to decide which explanation is correct, we took advantage of a possibility of modifying the geometry of the porphyrin inner cavity towards the core structure being nearly porphycene-like. Here, conformationally designed nonplanar porphyrins offer an intriguing possibility as model compounds.[4, 28, 29] It has been shown that the cavity becomes rectangular upon substitution, either by aryl or alkyl groups, at the opposite *meso* positions. This feature is characterized by the so-called core elongation factor.[4, 30] This is the case, e.g., for 5,15-diphenylporphyrin[31, 32] or 5,15-di-*n*-butyl-2,3,7,8,12,13,17,18-octaethylporphyrin.[33] In the latter, the N-N distance of 264 pm is practically the same as in porphycene.

In this work, we compare the spectral, photophysical, hydrogen-bonding, and tautomeric properties of two isomeric *meso*-substituted octaethylporphyrins: 2,3,7,8,12,13,17,18-octaethyl-5,15-

diphenylporphyrin (**1**) and 2,3,7,8,12,13,17,18-octaethyl-5,10-diphenylporphyrin (**2**) (Scheme 1). Starting with geometry optimizations, we show first that the two compounds have very different geometries; in particular, **1** is nearly planar, but **2** is not. While this difference is of rather minor importance for the electronic absorption, its influence on photophysics is considerable. A crucial finding is provided by comparing the tautomeric properties of **1**, possessing porphycene-like cavity, with those of **2**, with porphyrin-like geometry. We demonstrate that the two internal hydrogen atoms in **1** undergo, in the first elecronically excited state, tautomerization occuring on a nanosecond time scale. Thus, it is possible, by an appropriate distortion of the inner cavity, to speed up tautomerization in porphyrins by many orders of magnitude.

Results and Discussion

1. *Ground state geometry*

Previous structural studies of differently *meso*-substituted 2,3,7,8,12,13,17,18-octaethylporphyrins, including **1** and **2**, demonstrated that it is possible to change the type of distortion of the porphyrin skeleton, from in-plane to out-of-plane, by going from the 5,15- to the 5,10-diaryl substitution pattern.[35] Our present calculations corroborate this conclusion. Optimization of the ground state structures was performed not only for **1** and **2**, but also for model compounds, in which the ethyl substituents were replaced by methyl groups. This was done to check the possibility of complications due to various conformers with different relative positions of the ethyl groups. Similar results were obtained for both ethyl and methyl derivatives, the only exception being the transition moment directions of extremely weak S_0-S_1 and S_0-S_2 electronic transitions, discussed below in more detail.

As shown in Figure 1, the optimized geometries are very different for 5,15- and 5,10-diphenyl-substituted derivatives. The former is nearly planar, with the inner cavity shape that deviates strongly from a square, typical for porphyrins. The rectangular cavity with the NH⋯N distances of 269 pm is typical for porphycenes. In differently substituted porphycenes the values of NH⋯N distances span a range from 253 to 280 pm.[7] A consequence of the rectangular cavity shape is a more linear HB: the NHN angle is 129°, significantly larger than 116° in porphyrin.[21] Thus, one can expect much stronger intramolecular HBs in **1** than in the parent porphyrin and related derivatives such as 2,3,7,8,12,13,17,18-octaethylporphyrin (OEPr)[36] or 5,10,15,20-tetraphenylporphyrin (TPP).[37, 38] In all three compounds, the inner cavity has a square shape of practically the same dimensions. On the other hand, 5,15-diphenylporphyrin, carrying only two substituents, has a rectangular cavity with dimensions of 275 and 306 pm.[31] Similar pattern, a 264×326 pm² cavity is observed for 5,15-dibutyl-2,3,7,8,12,13,17,18-octaethylporphyrin.[33] We conclude that the distortion of the cavity from square to a rectangle can be achieved by double aryl or alkyl substitution at the opposite *meso* positions.

The geometry of the other, 5,10-diphenyl-substituted isomer **2** is completely different. The cavity is square-like, similar in size to an undistorted porphyrin, but the macrocycle becomes nonplanar, assuming a saddle shape. The largest out-of-plane deviation is observed for the pyrrole unit which has two phenyl substituents at the adjacent *meso* positions.
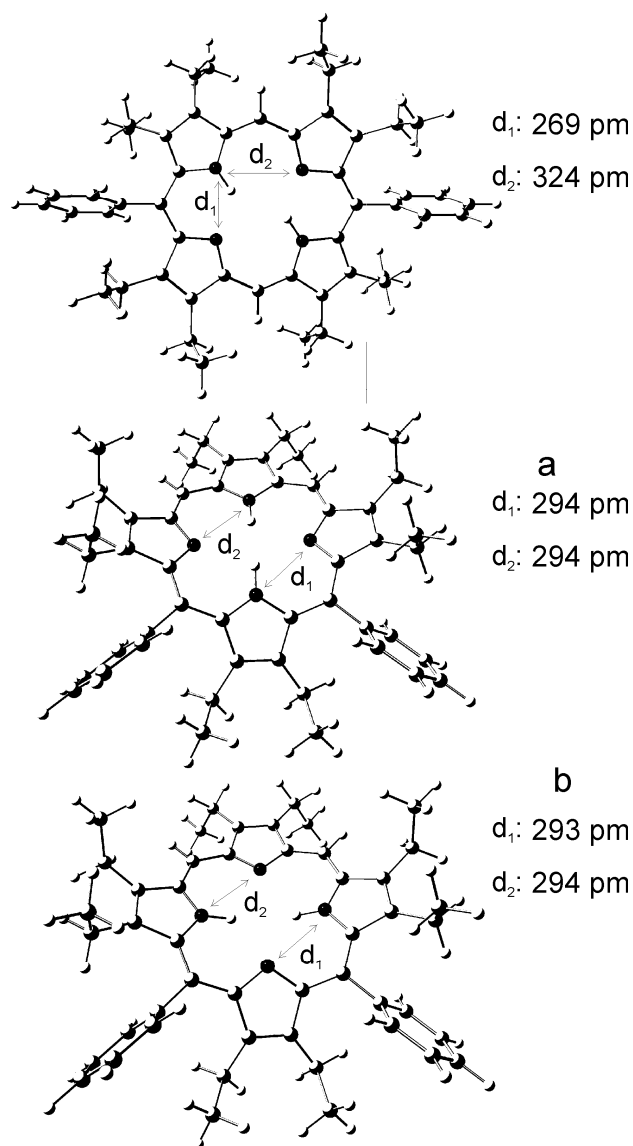
2

d₁: 269 pm
d₂: 324 pm

a
d₁: 294 pm
d₂: 294 pm

b
d₁: 293 pm
d₂: 294 pm

Figure1. B3LYP/6-31G(d,p) optimized ground state geometries of model compounds for **1** and **2**.

For both isomers, the lowest energy tautomeric forms correspond to *trans* structures, with the inner hydrogens located on the opposite pyrroles. The energy of *cis* forms, with protons on adjacent pyrroles is calculated to be about 4 kcal/mol higher for 5,15- and 8 kcal/mol for the 5,10-derivative. One should note that for the latter, two nonequivalent *trans tautomeric* species, **2a** and **2b**, are possible. Calculations for both forms yield very similar geometries (Figure 1) and energies. The two tautomers are practically degenerate; when zero-point-energy corrections are included, form **b** is predicted to be more stable by 0.5 kcal/mol.

Experimental X-ray data are available for **2**.[35] The agreement with present calculations is very good, the differences between experimental and calculated bond lengths not exceeding 1-2 pm. Slightly larger differences are observed for distances between the N atoms of the inner cavity. The theory (form **b** in Figure 1) predicts the N•••N values to be about 3 pm longer than obtained from crystal

structure analysis. However, the crystal data refer to a solvate complex of **2** and dichloromethane, involving two intermolecular hydrogen bonds between the hydrogen atoms of CH_2Cl_2 and the opposite nitrogen atoms of the inner cavity. As discussed later in this work, the propensity of **2** to coordinate protic solvents was confirmed by the analysis of fluorescence spectra in solutions.

Different geometries, regarding both planarity and hydrogen bond parameters indicate the possibility of different spectral, photophysical and tautomeric properties. The experiments probing these aspects of **1** and **2** are discussed in the next sections.

2. *Electronic spectroscopy*

Figure 2 shows the electronic absorption spectra of **1** and **2** compared with those of related porphyrins: Pr, OEPr, and TPP. Table 1 contains the comparison of experimental and calculated transition energies.
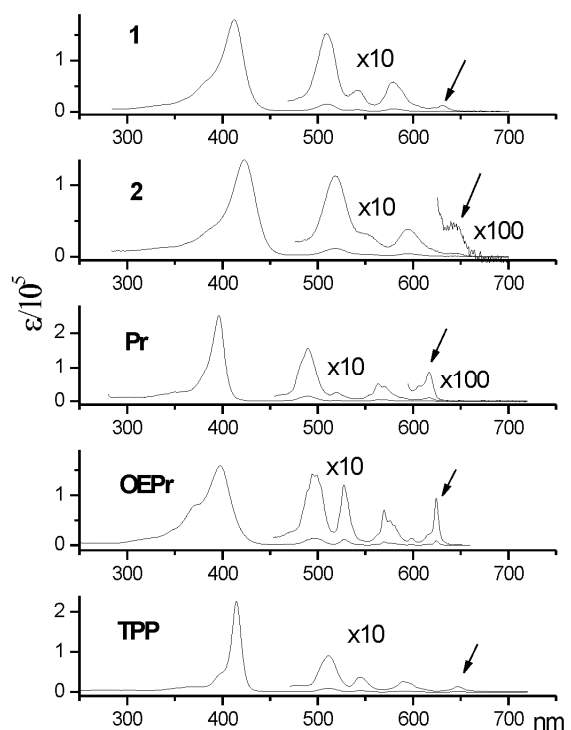

Figure 2. Room temperature absorption spectra recorded in toluene (**1**, **2**, Pr) or *n*-hexane (OEPr, TPP) solutions. The arrows show the origin of the S_0-S_1 transition.

The spectra of **1** and **2** exhibit very similar features. In the low energy region, they strongly resemble the spectrum of parent porphyrin, with a characteristic pattern of the S_1 and S_2 origin bands weaker than the respective higher energy vibronic components. In the higher energy (Soret) region, the absorption resembles that of OEPr, with a shoulder on the high energy side indicating a presence of a second electronic transition. The overall intensity of the Soret bands is similar in all the investigated porphyrins, as smaller values of the absorption coefficient at the maximum are compensated by larger bandwidths.

3

A red shift with regard to Pr is observed in **1** and **2** for the S_1 and S_2 transitions; the shifts are definitely larger for **2**. The relative values of the shifts are well reproduced by TD-DFT calculations, even though they overestimate the energy of the S_0-S_1 transition by 2000 cm^{-1} (Table 1).

Table 1. Relative transition energies with respect to porphyrin (red shift, cm^{-1}).

	S_0-S_1		S_0-S_2		calc osc. strength	
	exp	calc	exp	calc	S_0-S_1	S_0-S_2
Pr	0(16234)	0(18374)	0(19249)	0(19675)	0.0000	0.0000
1	412	644	696	843	0.0019	0.0040
2a	706	1213	1067	1408	0.0003	0.0059
2b	706	1325	1067	1359	0.0026	0.0019
TPP	766	1085	967	1188	0.0228	0.0416
OEPr	170	295	363	378	0.0050	0.0103

The electronic spectra of porphyrins can be analyzed using the simple four-orbital model of Gouterman,[39] or a related perimeter model approach developed by Michl.[40] A small ratio of the intensity of the low energy Q (L) bands with respect to the higher energy Soret (B) transitions is due to the near equality of the values of energy splittings between the two highest occupied molecular orbitals (ΔHOMO) and the two lowest unoccupied ones (ΔLUMO). In Michl's terminology, such chromophores are called "soft". The $|\Delta$HOMO $- \Delta$LUMO$|$ value calculated for **1** is 0.03 eV; for **2a** and **2b** one obtains 0.08 and 0.03 eV, respectively. These values are even lower than 0.12 eV, predicted for the parent porphyrin. In contrast, for porphycene, $|\Delta$HOMO $- \Delta$LUMO$| = 1.27$ eV and the calculated oscillator strengths are 0.129 and 0.197 for the S_0-S_1 and S_0-S_2 transitions, respectively. These values are about two orders of magnitude higher than those obtained for **1** and **2** (Table 1). Porphycene is a so-called "negative hard chromophore", with $|\Delta$HOMO$| \ll |\Delta$LUMO$|$. Such a pattern of frontier orbital splittings leads to comparable absorption intensities in the Q and Soret regions. Another consequence is a different intensity pattern of magnetic circular dichroism (MCD) spectra.[41] The MCD signal for porphycenes is stronger in the Q than in the Soret region. On the other hand for porphyrins, the MCD follows the absorption intensity pattern, i.e., a weak signal in the Q region is followed by a strong one in the region of Soret bands.

The MCD spectra of **1** and **2** are presented in Figure 3. The spectra are very similar, exhibiting a typical porphyrin-like pattern. A +,-,+,- sequence of MCD *B* terms is observed for the Q and Soret

bands (the negative MCD signal corresponds to a positive *B* term and vice versa). According to the perimeter model, such a pattern should be observed for $|\Delta$HOMO$| > |\Delta$LUMO$|$. Indeed, the calculations predict $|\Delta$HOMO$|$ and $|\Delta$LUMO$|$ values of 0.06 and 0.03 eV for **1**. The corresponding values are 0.14 and 0.06 eV for **2a**, and 0.10 and 0.07 eV for **2b**.

The MCD spectra reveal the presence of several electronic transitions on the blue side of the Soret bands. TDDFT calculations yielded 20 electronic transitions for wavelengths longer than 300 nm, several with oscillator strengths 0.1-0.3, intermediate between those of Q and Soret transitions (Supporting Information). Interestingly, some of these transitions are predicted to lie between the Q and Soret bands, red-shifted from the latter by 20-30 nm. No clear evidence for such ordering can be found in both absorption and MCD spectra, except perhaps a weak negative MCD signal in the region 450-500 nm.

On the basis of absorption and MCD measurements and TDDFT calculations one can conclude that both **1** and **2** retain the electronic structure of Pr, and neither the change in geometry of **1** towards a porphycene-like cavity nor a distortion from planarity in **2** do not significantly influence the pattern of electronic absorption. However, as discussed below, this does not imply that the directions of the electronic transition moments in **1** and **2** are the same as in Pr.
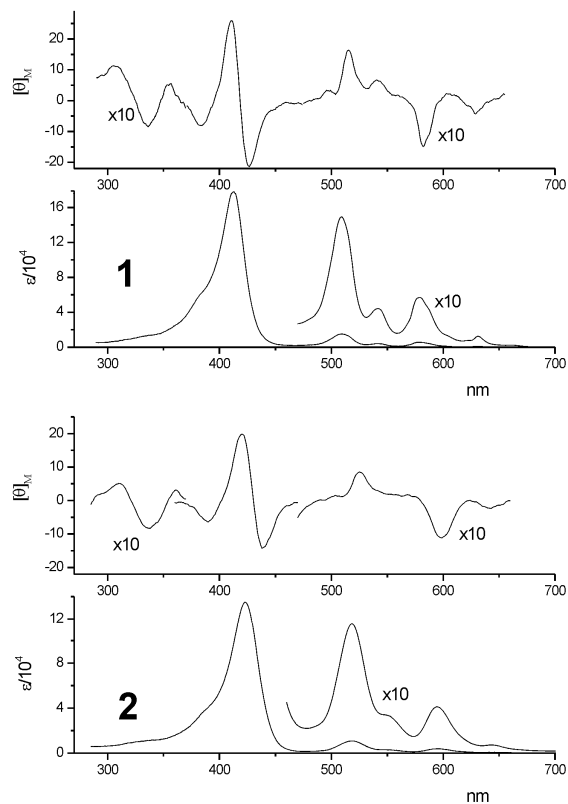

Figure 3. MCD spectra of **1** and **2** recorded at 293 for toluene solutions.

4

3. *Photophysics*

Fluorescence spectra of **1**, **2**, and those of related porphyrins Pr, OEPr, and TPP are shown in Figure 4. The spectra differ significantly in the ratio of the intensity of the 0-0 band to that of vibronic components observed at lower energies. This ratio can be treated as a measure of the allowed character of the electronic transition: the stronger the relative intensity of the vibronic features, the larger is the contribution from the vibronic coupling mechanism. Both **1** and **2** resemble the parent porphyrin in having a relatively low intensity of the 0-0 transition. This is in line with the behavior observed for the absorption and in agreement with low values of $|\Delta HOMO - \Delta LUMO|$ and the S_0-S_1 oscillator strength calculated for both compounds. A quantitative comparison is presented in Table 2, which shows the values of radiative and nonradiative rate constants obtained from fluorescence quantum yields and decay times. Compounds **1** and **2** exhibit the lowest values of the radiative rate constants, about twice smaller than Pr, for which the value is, in turn, about half that of TPP and OEPr. This sequence agrees nicely with the results of calculations which predict that the frontier π orbital HOMO and LUMO splittings in **1** and **2** are very similar; even more similar than for parent porphyrin. As discussed above, these compounds represent the "soft chromophores", for which the sign of $|\Delta HOMO - \Delta LUMO|$ can be readily reversed, e.g., by substitution, but also by minor perturbations, such as, e.g., shifts in tautomeric equilibria or a change in the environment. These changes in orbital splittings are reflected in the absorption, fluorescence, and, especially, in magnetic circular dichroism spectra, which can change sign along with $\Delta HOMO - \Delta LUMO$. Both **1** and **2**, approaching closely an ideal of a perfectly soft chromophore ($\Delta HOMO - \Delta LUMO = 0$), can thus be considered as potential sensors.

The nonradiative properties of **1** and **2** differ significantly. While the lowest excited singlet state of **1** is depopulated with approximately the same rate as in Pr, TPP, and OEPr, the other isomer exhibits a threefold increase in the sum of nonradiative rates. This can be related to nonplanarity, which often leads to such an enhancement, usually by accelerated internal conversion,[42] but sometimes also by enhanced intersystem crossing.[43] Interestingly, the fluorescence decay time of **2** does not change much in different environments, in particularly those with very different viscosities. This indicates no significant geometry changes upon excitation, at least not those involving large amplitude motions.

An interesting feature was observed for **2**, mainly for protic environments, but also for solvents containing hydroxylic impurities: both absorption and fluorescence change, and the emission decay becomes biexponential (Table 2). We attribute this behavior to ground state protonation of **2**, as these changes can be prevented by adding bases to the solution. This finding fits a previous observation that **2** in the crystal phase can doubly hydrogen bond, via its nitrogen atoms, to dichloromethane.[35]

The propensity of nonplanar porphyrins to undergo N-H hydrogen bonding is related to two factors. In saddle distorted porphyrins the N-H vectors are tilted out of the plane of the macrocycles, making them more accessible for H-acceptors.[44] This in contrast to the ruffled meso alkylporphyrins, where a tilt about the β-β axis leaves the N-H units in the core plane.[45, 46] Secondly, saddle distortion results in an increase in basicity by several orders of magnitude.[47, 48] Both factors have been implicated in the action of the natural metal inserting enzymes ferrochelatase and magnesium chelatase.[49, 50]
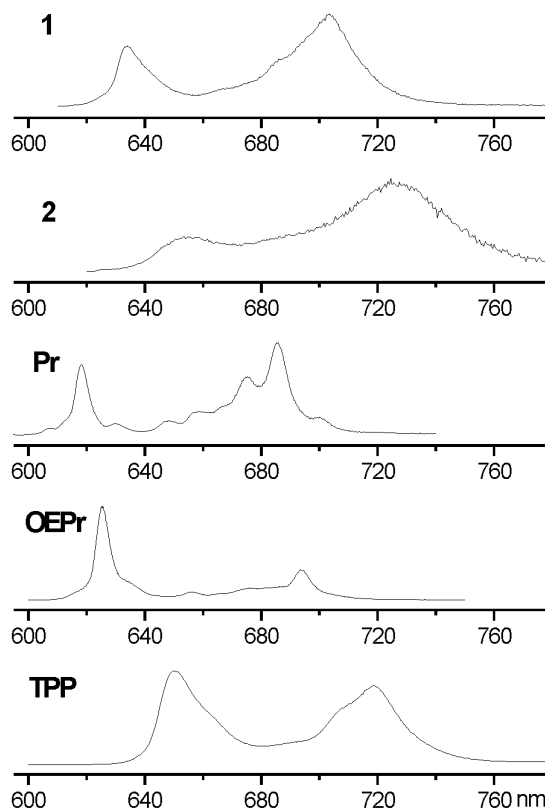

Figure 4. Fluorescence spectra of **1**, **2** and related porphyrins: Pr, OEPr, and TPP, recorded for toluene solutions at 293 K.

Table 2. Photophysical parameters of **1**, **2** and related porphyrins.

	Φ_{fl} [a]	τ_{fl} [b] [ns]	k_r [c]	$\sum k_{nr}$ [d]	Solvent
1	$(2.6\pm0.5)\cdot10^{-2}$	9.0±1.0 9.4±0.5 9.0±0.5 9.5±1.5 9.2±1.0	0.29	10.8	BuOH Toluene THF PS PVB
2	$(6.3\pm1.2)\cdot10^{-3}$ $(6.0\pm1.2)\cdot10^{-3}$ $(4.5\pm1.2)\cdot10^{-3}$	3.5±0.2 2.9±0.3 0.3-0.4/3.5±0.3 0.4-0.6/3.6±0.3	0.18 0.21	28.4 34.3	*n*-Hexane THF BuOH PVB
TPP	$7.5\cdot10^{-2}$	9.0	0.83	10.3	PrOH [77]
OEPr	0.16	21.7	0.74	3.9	Toluene [43]
Pr	$4.3\cdot10^{-2}$	9.6	0.45	10.0	Toluene [77]
Pc	0.36 0.36	10.2 10.7	3.5 3.4	6.3 5.9	Toluene [78] *n*-Hexane [20]

[a] fluorescence quantum yield at room temperature; [b] fluorescence decay time at room temperature; [c] radiative constant of S_1 depopulation; [d] sum of nonradiative constants

4. Hydrogen bonding and tautomerism

Different geometries of **1** and **2** suggest differences in the strength of the intramolecular HBs in the two molecules. Figure 5 shows a comparison of their IR spectra. For **2**, a band appearing at 3325 cm^{-1} can readily be assigned to the NH stretching vibration. The corresponding transition for Pr is observed at the same location, 3320-3330 cm-1.[51] The spectrum of **1** is significantly different, as no obvious candidate for the NH stretching band is observed. Replacement of the inner protons by deuterons results in the appearance of a band at 2352 cm^{-1}, assigned to the ND stretch. Simultaneously, a band disappears at 3101 cm^{-1}, indicating the location of the NH stretch in undeuterated **1**. This location is characteristic for strong HB. The behavior of **1** is somehow reminiscent of porphycene, where no such band was identified, even though the calculations suggested that it should be the strongest in the whole spectrum.[52] Calculations for **1** and **2** predict the transitions at 3273 and 3427 cm^{-1}, respectively (with the scaling factor of 0.96), the difference of 150 cm^{-1} clearly indicating much stronger HBs in the in-plane-distorted structure. Similarly to porphycene, the NH stretching band of **1** is calculated as the strongest in the IR spectrum. Note that for porphycenes the calculations predict much lower transition energies for the NH stretching, below 3000 cm^{-1}. Tautomerization in porphycenes occurs with rates ranging from tens of femtoseconds to hundreds of picoseconds.[24] The question now is to what degree the tautomerization rates are modified by strengthening of hydrogen bonds due to the in-plane inner cavity distortion: In **1**, the HBs are still weaker than in porphycenes, but definitely stronger than in typical porphyrins. In order to solve this problem, we used a methodology developed for the determination of the tautomerization rates in porphycenes.[20, 24, 53-56] It is based on the observation that intramolecular double hydrogen transfer leads to the rotation of transition moments by an angle dictated by their directions in the two chemically equivalent *trans* tautomers (Figure 6). Tautomerization can thus be monitored using spectroscopy with polarized light, by detecting the rotation of the transition moment under conditions when all other possible sources for its rotation, such as rotational diffusion or energy transfer, are excluded. This is done by recording the spectra of dilute solutions of molecules embedded in a rigid environment, e.g., a polymer film, glass, or a solidified gas. Both stationary and time-resolved techniques can be used. The former, based on the analysis of the emission anisotropy (*r*) can yield information about the tautomerization rates in the electronically excited state.[55] The same information is obtained from measurements of time-resolved fluorescence anisotropy. When the anisotropy is measured using pump-probe transient absorption technique, it is possible to simultaneously determine both ground and excited state tautomerization rates.[24, 56]

We have measured the steady-state anisotropy of fluorescence of **1** in various matrices: poly(vinyl butyral) and polystyrene films, glassy matrices of 3-methylpentane, 1-propanol, and 1:1 mixture of methanol:ethanol, as well as solutions using a very viscous solvent, castor oil. The latter has been previously used for measurements of fluorescence polarization of TPP. It was demonstrated that the viscosity of castor oil is sufficient to lengthen the time of the rotation of TPP to a value at least 50 times longer than the fluorescence lifetime.[57]
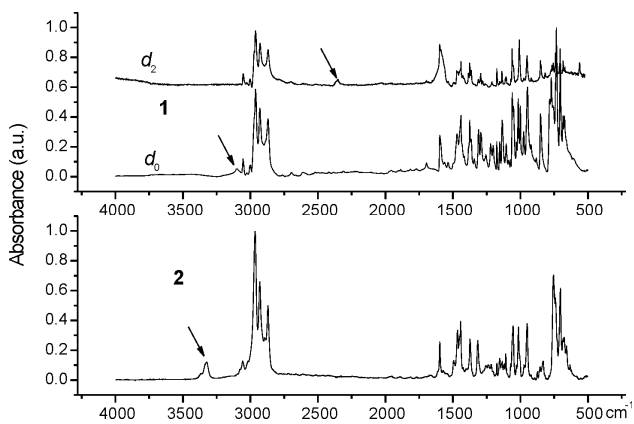

Figure 5. IR spectra of films of **1** and **2** recorded at 293 K. The arrows show the location of the NH stretch band.
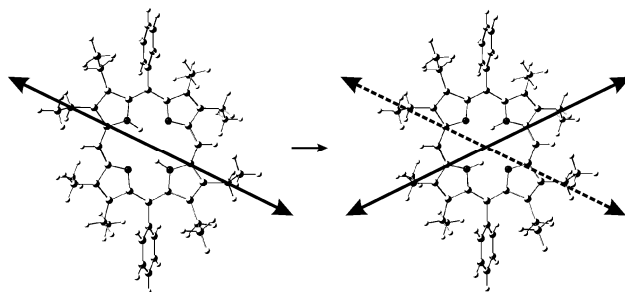

Figure 6. Illustration of TM direction (double-headed arrow) change as a result of intramolecular double hydrogen transfer. To visualize the angle between the TM directions in the reactant and product, the dashed arrow representing the TM position in the reactant is drawn over the product.

The emission anisotropy over the whole fluorescence region and the anisotropy of fluorescence excitation have been recorded, the latter for excitations wavelengths spanning a region of both Q and Soret transition. The general observation is that the anisotropy values vary very little for different excitation and emission wavelengths (Figure 7). The largest values, $r \approx 0.2$ were obtained for excitation into S_1 and monitoring the emission as close to the excitation as possible, usually about 10 nm. For all other combinations of excitation/emission wavelengths the anisotropy values are lower, spanning the range of 0.0 − 0.10, but never dropping below zero. Such pattern is strongly suggestive of depolarization. The value of 0.2, observed for **1** upon excitation to S_1, can be explained assuming that for some of the emitting molecules the TM directions are not the same in absorption and emission. This is due to the *trans-trans* conversion occurring in S_1. If the reaction is much faster than 10 ns S_1 lifetime, the angle between the S_0-S_1 TM directions in the two trans forms can be estimated as 55°. One should recall that if the TM directions coincide, no depolarization should occur, and the expected anisotropy value is 0.4. The other extreme, orthogonal TM directions in the two tautomers lead to $r = 0.1$. If the tautomerization is slower or comparable to the S_1 lifetime, depolarization is only partial, and the estimated value of the angle provides a lower limit. In free base porphyrin, the transition moments of both Q and Soret transitions are mutually orthogonal, the symbols Q_x and Q_y indicate

6

polarization along the NH – HN direction and the polarization perpendicular to it, respectively. For the case of non-overlapping transitions one should thus observe the emission anisotropy varying in the range -0.2 – 0.4. In particular, excitation into S_1 should yield high anisotropy values. One should remember, however, that in the case of porphyrin, the S_0-S_1 transition gains intensity via both Franck-Condon and Herzzberg-Teller contributions,[58-60] and the emission anisotropy pattern is quite complicated, with differently polarized vibronic bands overlapping each other.[61-63] Therefore, the low degree of anisotropy observed for **1** cannot, by itself, be considered as a definitive proof of excited state tautomerization.
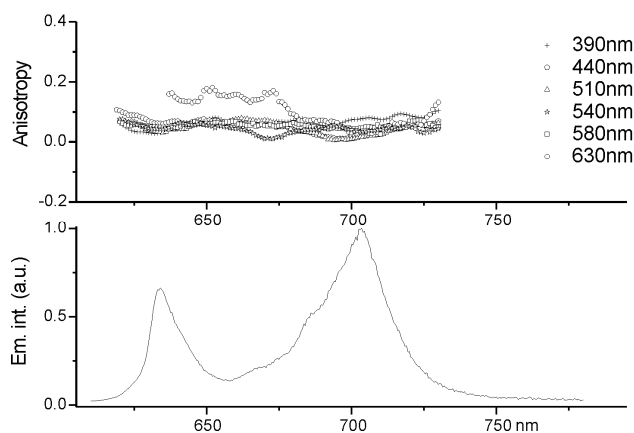

Figure 7. Anisotropy of fluorescence recorded at 293 K for **1** in castor oil using various excitation wavelengths: 630 (circles), 580 (squares), 540 (stars), 510 (triangles), 440 (pentagons), and 390 nm (crosses).

Figure 8 shows the transition moment directions calculated for **1** and for the octamethyl analogue. For the two strongly allowed Soret transitions, calculated as the 7-th and 8-th lowest excited singlet states, the positions of transition moments are very similar to those in the unsubstituted porphyrin: one of them (S_8) lies along the NH-HN direction, the other one (S_7) is perpendicular to it. However, this is not the case for the moments of low energy Q transitions. In porphyrin, they lie along the same in-plane directions, as the Soret transitions. For **1**, other directions are predicted. Moreover, quite different directions are calculated for ethyl- and methyl derivatives. Finally, contrary to the situation in Pr, it is now the second and not the lowest excited singlet state for which the transition moment lies closer to the NH-HN direction. Given the extremely small oscillator strength of the two lowest transitions, the calculated transition moment directions cannot be considered reliable.
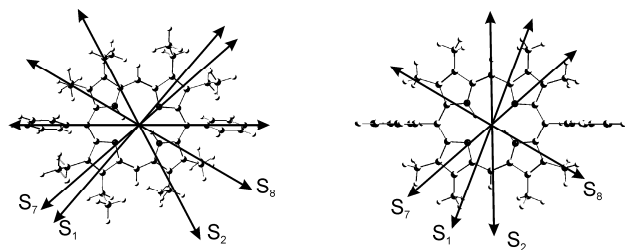

Figure 8. Transition moment directions of the Q (S_1, S_2) and Soret(S_7, S_8) bands calculated for **1** (left) and for its octamethyl substituted analogue (right).

For **2**, the situation is even more complex due to nonplanarity. The transition moment directions can now assume any orientation. The directions calculated for **2a** and **2b** are presented in Figure 9. For **2a**, the porphyrin-like TM directions are preserved for the Soret transitions, but this is no longer the case for **2b**.
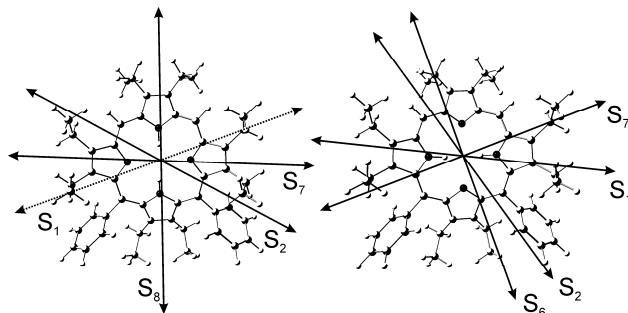

Figure 9. Transition moment directions of the Q (S_1, S_2) and Soret (S_7, S_8) bands calculated for two trans tautomers of **2**. The Soret bands correspond to S_7 and S_8 in the form **a** and to S_6 and S_7 in the form **b**. The dashed arrow indicates a TM with a large out-of-plane component.

Thus, while the analysis of the stationary fluorescence anisotropy of **1** strongly suggests tautomerization, it is not conclusive. Even though such a situation is highly unlikely, one cannot, in general, exclude an arrangement of TM directions leading to low and constant anisotropy values. In turn, a low value for S_1 excitation could, in principle, be due to the vibronic effects mentioned above. The definite proof of the reaction and the estimation of its rate were provided by time-resolved fluorescence measurements. In these experiments, temporal profiles of the fluorescence anisotropy were recorded in viscous environments (castor oil, polymer sheets) for excitation into S_1 (using picosecond 633 nm lasers). The anisotropy was obtained after measuring emission decays polarized in the direction parallel and perpendicular to the polarization of the excitation pulse: $r(t) = (I(t)_{par} - I(t)_{perp})/(I(t)_{par} + 2I(t)_{perp})$. The results are presented in Figure 10. One can immediately see the difference between the behavior of **1** and that of **2** and TPP, two porphyrin derivatives for which the excited state tautomerization should be much slower, and thus nonefficient on the time scale of 10 ns, i.e., the S_1 lifetime of **1**. For **2** and TPP, only a small decrease of the anisotropy is recorded over the temporal range spanning four fluorescence lifetimes. In contrast, the anisotropy of **1** decays in about 10 ns, reaching a plateau with $r \approx$ 0.1 for the PVB sample and a slightly lower value for the solution in castor oil. The finding that the anisotropy of **1** does not decay to zero is exactly as expected for the mechanism of depolarization involving excited state trans-trans conversion. In this model, tautomerization should evolve as

$$r(t) = \tfrac{1}{2}[r_1+r_2+(r_1-r_2)e^{-2kt}] \tag{1}$$

where r_1 and r_2 are the anisotropy values of the initially excited form and of the tautomer formed in the excited state; r_2 is thus determined by the angle between TMs in the two forms; the observed values of about 0.1 for the anisotropy plateau indicate that the S_0-S_1 transition moments are orthogonal in the two *trans* forms, similarly to the situation in the parent porphyrin. Formula 1 enables the estimation of k, the rate constant for excited state

tautomerization; its value is assumed to be the same for forward and back hydrogen transfer, since the two forms are chemically equivalent. Analysis of the anisotropy decay leads to the value of $k = 5(\pm1)\times10^7$ s^{-1}. It is known that direct fitting of the anisotropy should rather be avoided, due to improper propagation of errors.[64] Instead, one should rather use $I(t)_{par}$ and $I(t)_{perp}$, the experimentally obtained emission decays. However, the accurate analysis was not easy due to several factors. First, the tautomerization and the S_1 decay rates are comparable, which makes their separation rather difficult. For solution samples, even as viscous as castor oil, we could not totally avoid a contribution from rotational relaxation. This was probably caused by small fraction of a nonviscous solvent present, as the chromophores were introduced into castor oil from concentrated toluene solution. The rotational diffusion could be avoided for polymer samples, but now the concentration was much larger, with a possibility of depolarization by energy transfer. Finally, for some samples the decays, measured under magic angle conditions, were not strictly monoexponential. All in all, it seems safe to say that excited state tautomerization in **1** occurs at 293 K on a time scale of 10 ns.
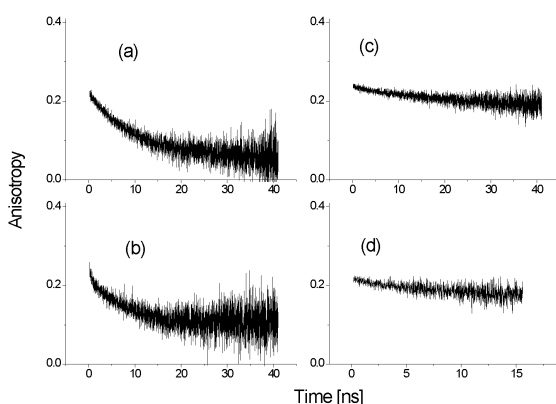

Figure 10. Time-resolved anisotropy profiles, monitored at 660 nm: (a) **1** in castor oil; (b) **1** in PVB sheet; (c) TPP in PVB sheet; (d) **2** in castor oil. All measurements were performed at 293 K.

A comment seems appropriate about using not only **2**, but also TPP as a reference compound in anisotropy studies. At first, **2**, as the isomer of **1**, could be considered an ideal reference. However, this chromophore may not be appropriate for several reasons. First, as discussed above, there is no restriction as to the possible angles of TM directions. Second, the degree of nonplanarity of the molecule may not be preserved upon excitation, causing a concomitant change in the TM directions. Finally, while measuring the transition anisotropy of **2**, we could not always get rid of traces of a second emission, assigned to the protonated or hydrogen-bonded molecule. Therefore, as a second, independent reference in anisotropy measurements we selected TPP, which has practically the same inner-cavity dimensions as Pr and **2**. Moreover, fluorescence anisotropy of TPP using castor oil has been reported before.[57] Our measurements for TPP reproduced the earlier steady-state experiments. In time-resolved experiments, practically no fluorescence depolarization due to rotational diffusion was observed for polymer samples; for castor oil solutions, the anisotropy decay observed for TPP was much slower than for **1**. Since the latter has a larger hydrodynamical volume than TPP, one can exclude molecular rotation as the reason for low anisotropy values observed for **1**.

Summary and Conclusions

Experimental and theoretical studies of two isomeric *meso*-diphenyl-octaethylporphyrins reveal regiochemical substituent pattern-induced changes in structure, spectroscopy, photophysics, hydrogen bond and tautomeric properties with respect to those of the parent porphyrin. In most instances, these changes are very much different for the 5,15- and 5,10-diphenyl regioisomers. The geometries of **1** and **2** are both distorted from the structure of Pr, but in completely different ways. Porphyrin **2** is nonplanar, but the inner cavity shape and dimensions are similar as in Pr. In contrast, **1** is approximately planar, but the in-plane distortion leads to a rectangular cavity, with NH···N distances different from those of Pr and close to these of porphycene. This has significant consequences for the intramolecular hydrogen bonds, which for **1** become much stronger than those of Pr, whereas practically no change is observed upon going from Pr to **2**. A stronger hydrogen bond facilitates intramolecular hydrogen transfer: excited state tautomerization is observed in the lowest excited electronic state of **1**, occurring with a rate of about 5×10^7 s^{-1}. In the ground state, the rate may be even higher: in differently substituted porphycenes the tautomerization in S_0 is about an order of magnitude faster than in S_1, due to the expansion of the inner cavity upon excitation, leading to a weaker HB and thus a higher barrier for hydrogen transfer.[24] An analogous expansion has also been predicted by calculations for Pr in the S_1 and T_1 electronic states.[65]

We have optimized the transition state structure for the ground state *trans-cis* conversion in **1**. The calculated cis-trans energy difference is 3.90 kcal/mol (3.55 kcal/mol after including the zero-point-energy correction). The transition state has been located 9.1 kcal/mol higher than the trans minimum (6.2 kcal/mol after ZPE correction). The corresponding values for Pr are: 8.2(7.8) kcal/mol for the *cis-trans* energy difference[7] and 16.2(13.1) for the transition state energy.[66] Using the calculated transition state energy values, one can estimate the ratio of tautomerization rates in **1** versus Pr as 9×10^4, in reasonable agreement with the results of the present studies and earlier work on Pr.[27, 67]

Studies of **1** demonstrate that, by using appropriate substitution, it is possible to convert porphyrin into a structure which, regarding tautomeric properties, resembles porphycene rather than the parent isomer. This is also confirmed by the values of the *cis-trans* energy difference, 2.4(1.9) kcal/mol, and the TS energy, 4.9(1.6) kcal/mol, calculated for porphycene.[68] The synthesis of **1** thus created a possibility of observing tautomerization in the lowest excited singlet state of a porphyrin derivative. Thus far, the photoinduced tautomerization in porphyrins[69-73] involved the triplet electronic state. Since the tautomerization in porphyrins may be applied for information storage,[74] the present results may carry practical implications.

We note that the increase of HBs strengths and the ensuing larger tautomerization rate in an appropriately substituted porphyrin is due to the altered geometry, but not electron density distribution. The calculated values of atomic charges for the inner nitrogen and hydrogen atoms turned out to be very similar for Pr, Pc, **1**, **2** and their methyl analogues. No correlation was found between excess charge and NH-N distance. For instance, the calculated charges on the protonated nitrogen are -0.655*e*, -0.664e, and -0.682*e* for Pr, Pc, and **1**, respectively. The largest density is thus obtained for the compound with the intermediate value of NH-N separation.

The influence of the diphenyl substitution on the photophysics is also position-specific and can be related to the pattern of geometry distortion. While the fluorescence characteristics of **1** are very similar to those of Pr, this is not the case for **2**, which reveals a significant decrease of the emission quantum yield and lifetime in comparison to its isomer. This is due to the threefold increase of the nonradiative deactivation channel, most probably caused by the nonplanar character of the chromophore.

Interestingly, the radiative constants for both **1** and **2** are quite similar to that of the parent Pr. In addition, the fluorescence spectra of the three compounds are quite similar (Figure 4). However, this does not imply that the influence of substituents on the electronic structure is minor. One should note that the fluorescence spectra of both OEPR and TPP differ significantly from those of Pr, **1**, and **2**. Specifically, the 0-0 transitions are much stronger in OEPR and TPP, indicating a more allowed character of the transition. This is also confirmed by higher values of the radiative constants (Table 2). We conclude that the spectral similarity of the electronic transition patterns in Pr, **1**, and **2** has its origin in the compensation of the effects caused, on one hand, by the ethyl, and, on the other hand, by phenyl substitutents. The parameter which determines the allowed character of the electronic transition is the difference in the energy splittings between the HOMO and LUMO orbitals. Using the perimeter model for porphycene[41] and other porphyrin isomers, hemiporhycene[75] and corrphycene[76] we have previously shown that the ratio of the dipole strengths of the Q and Soret bands varies with $\Delta HOMO^2 - \Delta LUMO^2$. As discussed in more detail in the photophysics section, the radiative constants follow the same trend as $|\Delta HOMO - \Delta LUMO|$, the lowest values of this difference being calculated for **1** and **2**. Tuning of $|\Delta HOMO - \Delta LUMO|$, and thus of the strength of the electronic transitions in porphyrins, can be done more precisely by stepwise changing of the number of alkyl substituents. We will demonstrate this in a future work devoted to singly, doubly, triply and quadruply *meso-n-*hexyl-substituted porphyrins.

Experimental Section

The synthesis and purification of **1** and **2** have been described previously.[34, 35] Free base porphyrin (Pr, Frontier Scientific), 21*H*,23*H*-5,10,15,20-tetraphenylporphyrin (TPP, Aldrich), and 21*H*,23*H*-2,3,7,8,12,13,17,18-octaethylporphyrin (OEPr, Aldrich) were used as received.

The solvents (CCl₄, IR grade, toluene, tetrahydrofuran (THF), 1-butanol, and CHCl₃, spectroscopic grade, all from Merck, castor oil (Roth) were used without further purification. Samples of **1** and **2** embedded in a polymer films (poly(vinyl butyral-*co*-vinyl alcohol-*co*-vinyl acetate) (PVB, Aldrich, average molecular weight 90000-120000)) or polystyrene (POCH)) were obtained by casting from polymer solutions in THF or toluene.

The UV/VIS spectra were recorded on a Shimadzu UV-3100 spectrophotometer. Magnetic dicrcular dichroism (MCD) spectra have been obtained using an OLIS DSM 17 CD spectropolarimeter, equipped with a permanent magnet of 1.06 T field strength.

Fluorescence has been measured using either an Edinburgh FS 900 CDT or a Horiba Jobin Yvon Fluorolog-3 spectrofluorometers. Both instruments were equipped with polarizers for the measurements of stationary emission anisotropy. For quantum yield measurements, parent porphycene in *n*-hexane solution was chosen (Φ_{fl} = 0.36),[20] because of the emission spectral range, very similar to those of **1** and **2**.

Time-resolved fluorescence spectra have been recorded with a home-built setup, consisting of a Becker & Hickl BHL-600 (635 nm, 100 ps pulse) or an IBH picosecond diode (633 nm, 200 ps pulse) laser modules, a Digikröm CM112 monochromator working in the subtractive mode, a Becker & Hickl PMC 100-4 photomultiplier or an id100-20 id Quantique single-photon detection module. The signals were processed by a

Becker & Hickl SPC-830 time-correlated single photon counting module. For the analysis of fluorescence decays, we employed the FAST Advanced Analysis of Fluorescence Kinetics software (Edinburgh Instruments, version 3). The same setup, additionally equipped with a Glan-Thompson calcite polarizer, was used for time-resolved anisotropy measurements. Care was taken to ensure that the emission monochromator was properly calibrated to account for different responses to differently polarized light beams.

The infrared spectra were measured for solid **1** and **2** using a Nicolet Magna 560 spectrometer with an MCT/B liquid-nitrogen-cooled detector. The isotopomer of **1**, with the internal protons replaced by deuterons was obtained by dissolving the compound in CH₃OD/CHCl₃ mixture and subsequent evaporation of the solvent.

All the quantum-chemical calculations were performed using Gaussian 03 (Revision B.04) and Gaussian 09 (Revision A.02) packages, using the density functional theory (DFT), B3LYP functional, and 6-31G(d,p) basis set. Optimization of the ground state geometry was followed by calculation of vibrational frequencies. Electronic transition energies were calculated by time-dependent DFT (TDDFT), using S_0-optimized geometries as input.

[1] *Handbook of Porphyrin Science, Vol. 1-10*, K. Smith, K. Kadish, R. Guilard, Eds., World Scientific, Singapore, **2010**.

[2] C. M. Drain, S. Gentemann, J. A. Roberts, N. Y. Nelson, C. J. Medforth, S. L. Jia, M. C. Simpson, K. M. Smith, J. Fajer, J. A. Shelnutt, D. Holten, *J. Am. Chem. Soc.* **1998**, *120*, 3781-3791.

[3] B. Röder, M. Büchner, I. Rückman, M. O. Senge, *Photochem. Photobiol. Sci.* **2010**, *9*, 1152–1158.

[4] M. O. Senge, in *The Porphyrin Handbook, Vol. 1* (Eds.: K. M. Kadish, K. M. Smith, R. Guilard), Academic Press, San Diego, **2000**, pp. 239-347.

[5] J. L. Sessler, A. Gebauer, E. Vogel, in *The Porphyrin Handbook, Vol. 2* (Ed.: K. M. Kadish, Smith, K.M., Guilard, R.), Academic Press, New York, **2000**, pp. 1-54.

[6] J. L. Sessler, S. J. Weghorn, *Expanded, Contracted & Isomeric Porphyrins*, Elsevier, Oxford, **1997**.

[7] J. Waluk, in *Handbook of Porphyrin Science, Vol. 7* (Eds.: K. Smith, K. Kadish, R. Guilard), World Scientific, Singapore, **2010**, pp. 359-436.

[8] J. Waluk, J. Michl, *J. Org. Chem.* **1991**, *56*, 2729-2735.

[9] E. Vogel, M. Köcher, H. Schmickler, J. Lex, *Angew. Chem., Int. Ed. Engl.* **1986**, *25*, 257-259.

[10] H. J. Callot, B. Metz, T. Tschamber, *New J. Chem.* **1995**, *19*, 155-159.

[11] E. Vogel, M. Bröring, S. J. Weghorn, P. Scholz, R. Deponte, J. Lex, H. Schmickler, K. Schaffner, S. E. Braslavsky, M. Müller, S. Pörting, C. J. Fowler, J. L. Sessler, *Angew. Chem., Int. Ed. Engl.* **1997**, *36*, 1651-1654.

[12] M. A. Aukauloo, R. Guilard, *New J. Chem.* **1994**, *18*, 1205-1207.

[13] J. L. Sessler, E. A. Brucker, S. J. Weghorn, M. Kisters, M. Schafer, J. Lex, E. Vogel, *Angew. Chem., Int. Ed. Engl.* **1994**, *33*, 2308-2312.

[14] E. Vogel, M. Bröring, C. Erben, R. Demuth, J. Lex, M. Nendel, K. N. Houk, *Angew. Chem., Int. Ed. Engl.* **1997**, *36*, 353-357.

[15] E. Vogel, P. Scholz, R. Demuth, C. Erben, M. Broring, H. Schmickler, J. Lex, G. Hohlneicher, D. Bremm, Y. D. Wu, *Angew. Chem.-Int. Edit.* **1999**, *38*, 2919-2923.

[16] P. J. Chmielewski, L. Latos-Grażynski, K. Rachlewicz, T. Glowiak, *Angew. Chem., Int. Ed. Engl.* **1994**, *33*, 779-781.

[17] H. Furuta, T. Asano, T. Ogawa, *J. Am. Chem. Soc.* **1994**, *116*, 767-768.

[18] S. E. Braslavsky, M. Müller, D. O. Mártire, S. Pörting, S. G. Bertolotti, S. Chakravorti, G. Koç-Weier, B. Knipp, K. Schaffner, *J. Photochem. Photobiol. B: Biol.* **1997**, *40*, 191-198.

[19] J. C. Stockert, M. Cañete, A. Juarranz, A. Villanueva, R. W. Horobin, J. Borrell, J. Teixidó, S. Nonell, *Curr. Med. Chem.* **2007**, *14*, 997-1026.

[20] M. Gil, J. Dobkowski, G. Wiosna-Sałyga, N. Urbańska, P. Fita, C. Radzewicz, M. Pietraszkiewicz, P. Borowicz, D. Marks, M. Glasbeek, J. Waluk, *J. Am. Chem. Soc.* **2010**, *132*, 13472-13485.

[21] U. Langer, C. Hoelger, B. Wehrle, L. Latanowicz, E. Vogel, H. H. Limbach, *J. Phys. Org. Chem.* **2000**, *13*, 23-34.

[22] B. Chen, A. Tulinsky, *J. Am. Chem. Soc.* **1972**, *94*, 4144-4151.

[23] I. Saltsman, I. Goldberg, Y. Balazs, Z. Gross, *Tetrahedron Lett.* **2007**, *48*, 239-244.

[24] P. Fita, N. Urbańska, C. Radzewicz, J. Waluk, *Chem.- Eur. J.* **2009**, *15*, 4851-4856.

[25] M. Schlabach, B. Wehrle, H. Rumpel, J. Braun, G. Scherer, H. H. Limbach, *Ber. Bunsen-Ges. Phys. Chem.* **1992**, *96*, 821-833.

[26] J. Braun, M. Schlabach, B. Wehrle, M. Köcher, E. Vogel, H. H. Limbach, *J. Am. Chem. Soc.* **1994**, *116*, 6593-6604.

[27] J. Braun, H. H. Limbach, P. G. Williams, H. Morimoto, D. E. Wemmer, *J. Am. Chem. Soc.* **1996**, *118*, 7231-7232.

[28] M. O. Senge, *J. Photochem. Photobiol. B* **1992**, *16*, 3-36.

[29] M. O. Senge, *Chem. Comm.* **2006**, 243-256.

[30] C. J. Medforth, M. O. Senge, T. P. Forsyth, J. D. Hobbs, J. A. Shelnutt, K. M. Smith, *Inorg. Chem.* **1994**, *33*, 3865-3872.

[31] A. D. Bond, N. Feeder, J. E. Redman, S. J. Teat, J. K. M. Sanders, *Cryst. Growth Des.* **2002**, *2*, 27-39.

[32] Y. H. Zhang, Z. Y. Li, Y. D. Wu, Y. Z. Zhu, J. Y. Zheng, *Spectrochim. Acta A* **2005**, *62*, 83-91.

[33] M. O. Senge, W. W. Kalisch, I. Bischoff, *Chem.-Eur. J.* **2000**, *6*, 2721-2738.

[34] W. W. Kalisch, M. O. Senge, *Angew. Chem. Int. Ed. Engl.* **1998**, *37*, 1107-1109.

[35] M. O. Senge, I. Bischoff, *Eur. J. Org. Chem.* **2001**, 1735-1751.

[36] J. W. Lauher, J. A. Ibers, *J. Am. Chem. Soc.* **1973**, *95*, 5148-5152.

[37] S. J. Silvers, A. Tulinsky, *J. Am. Chem. Soc.* **1967**, *89*, 3331-3337.

[38] K. Kano, K. Fukuda, H. Wakami, R. Nishiyabu, R. F. Pasternack, *J. Am. Chem. Soc.* **2000**, *122*, 7494-7502.

[39] M. Gouterman, *J. Mol. Spectrosc.* **1961**, *6*, 138-163.

[40] J. Michl, *Tetrahedron* **1984**, *40*, 3845-3934.

[41] J. Waluk, M. Müller, P. Swiderek, M. Köcher, E. Vogel, G. Hohlneicher, J. Michl, *J. Am. Chem. Soc.* **1991**, *113*, 5511-5527.

[42] S. Gentemann, C. J. Medforth, T. Ema, N. Y. Nelson, K. M. Smith, J. Fajer, D. Holten, *Chem. Phys. Lett.* **1995**, *245*, 441-447.

[43] S. Gentemann, C. J. Medforth, T. P. Forsyth, D. J. Nuro, K. M. Smith, J. Fajer, D. Holten, *J. Am. Chem. Soc.* **1994**, *116*, 7363-7368.

[44] M. O. Senge, *Z. Naturforsch.* **1999**, *54b*, 821–824.

[45] M. O. Senge, *Z. Naturforsch.* **2000**, *55b*, 336-344.

[46] M. O. Senge, M. W. Renner, W. W. Kalisch, J. Fajer, *J. Chem. Soc., Dalton Trans.* **2000**, 381-385.

[47] O. S. Finikova, A. V. Cheprakov, P. J. Carroll, S. Dalosto, S. A. Vinogradov, *Inorg. Chem.* **2002**, *41*, 6944-6946.

[48] L. D. Sparks, C. J. Medforth, M.-S. Park, J. R. Chamberlain, M. R. Ondrias, M. O. Senge, K. M. Smith, J. A. Shelnutt, *J. Am. Chem. Soc.* **1993**, *115*, 581-592.

[49] S. Al-Karadaghi, M. Hansson, e. a. Nikonov S, B. Jönsson, L. Hederstedt, *Structure* **1997**, *5*, 1501-1510.

[50] J. Takeda, T. Ohya, M. Sato, *Inorg. Chem.* **1992**, *31*, 2877-2880.

[51] J. G. Radziszewski, J. Waluk, J. Michl, *Chem. Phys.* **1989**, *136*, 165-180.

[52] K. Malsch, G. Hohlneicher, *J. Phys. Chem. A* **1997**, *101*, 8409-8416.

[53] J. Waluk, E. Vogel, *J. Phys. Chem.* **1994**, *98*, 4530-4535.

[54] J. Waluk, *Acc. Chem. Res.* **2006**, *39*, 945-952.

[55] M. Gil, J. Waluk, *J. Am. Chem. Soc.* **2007**, *129*, 1335-1341.

[56] P. Fita, N. Urbańska, C. Radzewicz, J. Waluk, *Z. Phys. Chem.* **2008**, *222*, 1165-1173.

[57] J. W. Weigl, *J. Mol. Spectrosc.* **1957**, *1*, 133-138.

[58] B. Minaev, Y. H. Wang, C. K. Wang, L. Luo, H. Ågren, *Spectrochim. Acta A* **2006**, *65*, 308–323.

[59] M. Perrin, M. Gouterman, C. Perrin, *J. Chem. Phys.* **1969**, *50*, 4137-4150.

[60] A. T. Gradyushko, K. N. Solovev, A. Starukhin, *Opt. Spectrosc.* **1976**, *40*, 267-271.

[61] A. N. Sevchenko, K. N. Solov'ev, V. A. Mashenkov, S. F. Shkirman, *Dokl. Akad. Nauk SSSR* **1965**, *163*, 1367-1370.

[62] S. M. Arabei, S. K. Shkirman, K. N. Solovyov, G. D. Yegorova, *Spectrosc. Lett.* **1977**, *10*, 677-697.

[63] J. Radziszewski, J. Waluk, J. Michl, *J. Mol. Spectrosc.* **1990**, *140*, 373-389.

[64] J. R. Lakowicz, in *Principles of Fluorescence Spectroscopy*, Springer Science+Business Media, **2006**, p. 388.

[65] S. Perun, J. Tatchen, C. M. Marian, *ChemPhysChem* **2008**, *9*, 282-292.

[66] J. Baker, P. M. Kozlowski, A. A. Jarzecki, P. Pulay, *Theor. Chem. Acc.* **1997**, *97*, 59-66.

[67] H. H. Limbach, B. Wehrle, H. Zimmermann, R. D. Kendrick, C. S. Yannoni, *Angew. Chem. Int. Ed. Engl.* **1987**, *26*, 247-248.

[68] J. Waluk, in *Hydrogen-Transfer Reactions, Vol. 1* (Eds.: J. T. Hynes, J. P. Klinman, H. H. Limbach, R. L. Schowen), Wiley-VCH, Weinheim, **2007**, pp. 245-271.

[69] K. N. Solov'ev, I. E. Zalesski, V. N. Kotlo, S. F. Shkirman, *JETP Lett. (Eng. Transl.)* **1973**, *17*, 332-334.

[70] I. E. Zalesski, V. N. Kotlo, A. N. Sevchenko, K. N. Solov'ev, S. F. Shkirman, *Sov. Phys. Dokl. (Eng. Transl.)* **1973**, *17*, 1183-1185.

[71] S. Völker, J. H. van der Waals, *Mol. Phys.* **1976**, *32*, 1703-1718.

[72] S. S. Dvornikov, V. A. Kuz'mitskii, V. N. Knyukshto, K. N. Solov'ev, *Dokl. Akad. Nauk SSSR* **1985**, *282*, 362-366.

[73] J. G. Radziszewski, J. Waluk, M. Nepraš, J. Michl, *J. Phys. Chem.* **1991**, *95*, 1963-1969.

[74] A. Renn, U. P. Wild, A. Rebane, *J. Phys. Chem. A* **2002**, *106*, 3045-3060.

[75] A. Gorski, E. Vogel, J. L. Sessler, J. Waluk, *Chem. Phys.* **2002**, *282*, 37-49.

[76] A. Gorski, E. Vogel, J. L. Sessler, J. Waluk, *J. Phys. Chem. A* **2002**, *106*, 8139-8145.

[77] A. T. Gradyushko, M. P. Tsvirko, *Opt. Spectrosc. (Russ.)* **1971**, *31*, 548-556.

[78] P. F. Aramendia, R. W. Redmond, S. Nonell, W. Schuster, S. E. Braslavsky, K. Schaffner, E. Vogel, *Photochem. Photobiol.* **1986**, *44*, 555-559.
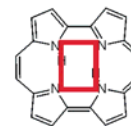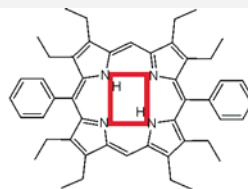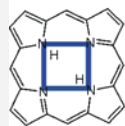
10

Entry for the Table of Contents

5,15-diphenyl substitution of octaethylporphyrin changes the geometry of the inner cavity. The resulting shape and dimensions resemble those of porphycene, a porphyrin isomer known for its strong intramolecular hydrogen bonds and ultrafast tautomerization.

In the appropriately substituted porphyrinoid, the tautomerization rate becomes several orders of magnitude larger than in the parent compound, but it is still significantly lower than in porphycene.